

Error-correction properties of an interacting topological insulator

Amit Jamadagni* and Hendrik Weimer

Institut für Theoretische Physik, Leibniz Universität Hannover, Appelstraße 2, 30167 Hannover, Germany

We analyze the phase diagram of a topological insulator model including antiferromagnetic interactions in the form of an extended Su-Schrieffer Heeger model. To this end, we employ a recently introduced operational definition of topological order based on the ability of a system to perform topological error correction. We show that the necessary error correction statistics can be obtained efficiently using a Monte-Carlo sampling of a matrix product state representation of the ground state wave function. Specifically, we identify two distinct symmetry-protected topological phases corresponding to two different fully dimerized reference states. Finally, we extend the notion of error correction to classify thermodynamic phases to those exhibiting local order parameters, finding a topologically trivial antiferromagnetic phase for sufficiently strong interactions.

The classification of topological phases beyond the Landau symmetry breaking paradigm remains an outstanding challenge in many-body physics since the discovery of the topological origin of the integer quantum Hall effect almost 40 years ago [1]. While the non-interacting case is well understood in terms of topological invariants [2], giving rise to a plethora of topological insulators and superconductors [3], counterexamples to successful classification can be found in the case of interacting systems [4].

More recently, many-body topological invariants have been proposed to classify one-dimensional phases with symmetry-protected topological (SPT) order [5–7]. However, the possibility to acquire nonzero values even for topologically trivial phases prevents a direct identification in terms of a topological order parameter, meaning that successful classification of phases requires a complete set of invariants [8]. To overcome these challenges, we have recently introduced an operational definition of topological order based on the ability of a system to perform topological error correction [9]. While the notion of topological error correction is chiefly motivated by quantum memories such as the toric code exhibiting intrinsic topological order [10], topological qubits based on Majorana fermions are also prominently found within one-dimensional topological superconductors [11–13], hinting at a possible generalization of the operational definition.

In this Letter, we apply the operational definition in the context of the Su-Schrieffer-Heeger (SSH) model [14], a paradigmatic model for a one-dimensional topological insulator [15], whose bosonic variant has also recently been realized experimentally using ultracold Rydberg atoms [16]. While the SSH model has so far not been discussed in the context of topological error correction, we show that such a formulation can be readily found by defining errors in terms of perturbations of the fully dimerized limits of the model. We discover two distinct types of errors, describing density and phase fluctuations, respectively, showing that only the former are necessary to describe the topological phase transition in the non-interacting case. We analyze the model numerically in terms of a Monte-Carlo sampling of the error correction

procedure based on a matrix product state (MPS) calculation of the ground state. In particular, we find that both phases of the noninteracting SSH model are topologically ordered, corresponding to two different choices of the unit cell, which is also supported by the appearance of distinct bulk topological invariants for the two choices. Finally, we consider an extension of the bosonic SSH model including antiferromagnetic interactions [7], where we see that SPT order persists for finite interaction strengths before an antiferromagnetic phase finally takes over.

SSH model.— We consider the hardcore boson variant of the SSH model with the Hamiltonian being defined on a 1D chain consisting of N spin-1/2 particles as

$$H_0 = v \sum_{i=1}^{N/2} \sigma_-^{2i-1} \sigma_+^{2i} + w \sum_{i=1}^{N/2-1} \sigma_-^{2i} \sigma_+^{2i+1} + \text{h.c.}, \quad (1)$$

with the spin creation and annihilation operators satisfying the commutation relation $[\sigma_-, \sigma_+] = \sigma_z$ in terms of the Pauli spin matrix σ_z . In the case of open boundary conditions, there is one w link less than there are v links, while for periodic boundary conditions, the number of links are equal for both types. In the latter case, the system is translational invariant and can be solved by mapping onto free fermions using a Jordan-Wigner transformation and partitioning the system into unit cells of two sites, which can be done in two different ways, see Fig. 1a. Since the model is invariant under exchanging the unit cell and exchanging v and w at the same time, fixing the unit cell is similar to fixing a gauge. For the AB unit cell, performing a Fourier transform gives rise to the band Hamiltonian $H(k) = d_x(k)\sigma_x + d_y(k)\sigma_y$ with $d_x(k) = v + w \cos k$ and $d_y(k) = w \sin k$, with the spin variable referring to the A and B sites of a single unit cell [15]. Its eigenenergies are given by $E(k) = |v + e^{-ik}w|$. From the energy spectrum we note that for $v < w$ and $v > w$, the band gap is finite resulting in insulating phases while at $v = w$ we have a conductor due to the closing of the band gap. We can see that this closing of the gap is due to the presence of a phase transition between distinct topological phases by considering two dif-

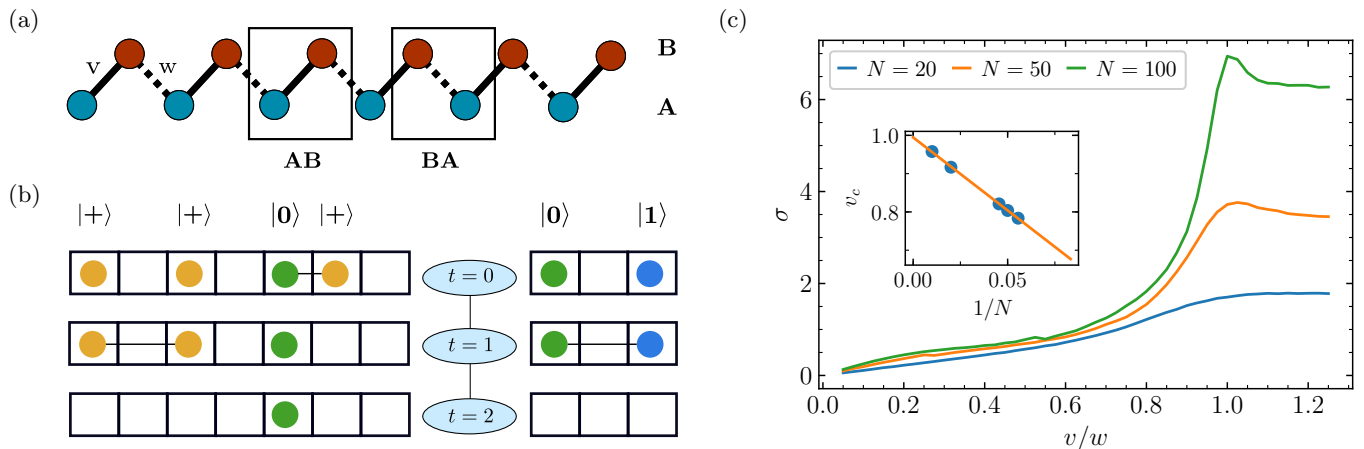


FIG. 1. (a) The SSH model can be understood as two alternating sites A and B coupled by bonds with interaction strength v and w , respectively. For periodic boundary conditions, there are two equivalent unit cells, denoted as AB and BA . (b) Error correction for the SSH model. First (left), phase fluctuations (yellow) are corrected by either fusing them pairwise or absorbing them into a density fluctuation. In the second stage (right), the remaining density fluctuation are removed by fusing holes (green) and particles (blue). Fusion operations at the step t are indicated by horizontal lines. The total circuit depth is the sum of the number of steps the two circuits require to return to the reference state. (c) Standard deviation σ of the circuit depth σ for the SSH model for the reference state $|\psi_{AB}\rangle$ for different system sizes. Finite size scaling of peak of the susceptibility $\chi_v = \partial\sigma/\partial v$ (inset) yields a critical value of $v_c/w = 1.00(1)$.

ferent topological invariants corresponding to the choice of the unit cell. Specifically, we consider the winding number

$$\nu = \frac{1}{2\pi i} \int_{-\pi}^{\pi} dk \frac{d}{dk} \log h(k) \quad (2)$$

where $h(k) = d_x(k) - id_y(k)$ [15]. Choosing the AB as the unit cell, we have $\nu_{AB} = 1$ for $v < w$ and $\nu_{AB} = 0$ for $v > w$. Due to the presence of the $v \leftrightarrow w$ symmetry, we immediately see that we have $\nu_{BA} = 0$ in the former and $\nu_{BA} = 1$ in the latter case.

Interestingly, the error basis can be also used to provide additional insight into the topological phase transition. Within perturbation theory in v/w (for the AB unit cell), we find that phase fluctuations correspond to higher order processes compared to density fluctuations. This means that we can neglect the $|+\rangle$ state in an effective low-energy description of the SSH model, arriving at a spin-1 representation according to

$$H_{\text{eff}} = \sum_i w S_i^z{}^2 + v (S_i^+ S_{i+1}^- + \text{H.c.}). \quad (3)$$

Here, w takes the role of an uniaxial anisotropy, while v describes a hopping of the spin excitations. Constructing such effective models for the dynamics of errors is reminiscent of effective Ising models describing the topological phase transition in perturbed toric code models [17, 18]. The phase diagram of this spin-1 model is well-known [19–21], exhibiting a phase transition between a large- w

phase corresponding to the fully dimerized limit and a Haldane insulator at $v/w = 1$. Note that the phase for $v > w$ is also topologically ordered; this is another manifestation of the $v \leftrightarrow w$ symmetry relating the two phases to each other.

Error correction properties.— Although the non-interacting SSH model is exactly solvable, it is instructive to numerically study its error correction properties, which will serve as a base to investigate the interacting case. For this, we turn to the operational definition of topological order [9], which relates the existence of a phase transition to the divergence of the depth of an appropriate error correction circuit with respect to a particular reference state. For the SSH model, the reference states can be readily identified as the ground states in the fully dimerized limit given by $v = 0$ or $w = 0$, respectively, i.e.,

$$|\psi\rangle_{AB/BA} = \frac{1}{\sqrt{2}} \prod_{i \in B/A} (|0\rangle_i |1\rangle_{i+1} - |1\rangle_i |0\rangle_{i+1}). \quad (4)$$

The errors with respect to these reference states can then be found by considering a complete basis of possible excitations. For a single bond between two unit cells, we can denote the error-free state as $|-\rangle = (|01\rangle - |10\rangle)/\sqrt{2}$. Additionally, we can identify particle and hole excitations indicated by the states $|1\rangle = |11\rangle$ and $|0\rangle = |00\rangle$, respectively, as well as phase fluctuations given by $|+\rangle = (|01\rangle + |10\rangle)/\sqrt{2}$. Repeating this procedure over the entire system will then define a unitary transformation allowing

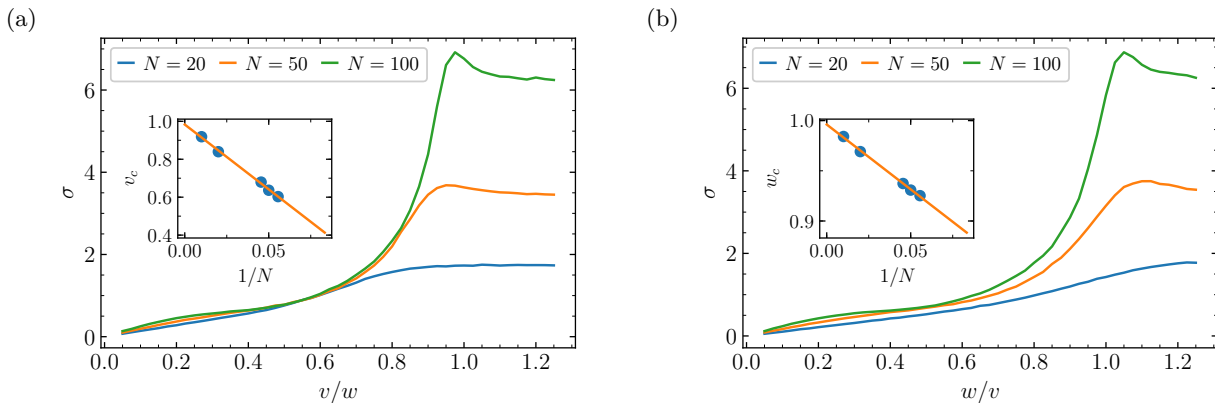


FIG. 2. Standard deviation σ of the circuit depth σ for the reference state $|\psi_{AB}\rangle$ (a) and $|\psi_{BA}\rangle$ (b). The insets show the finite size scaling resulting in $v_c/w = 0.98(1)$ and $w_c = 1.00(1)$, respectively.

us to express any state in this error basis.

Having specified the reference state and a complete set of errors, we now turn to the actual error correction procedure. In the following, we assume that the system has been measured in the error basis, yielding a classical string of errors. As the topological phases of the SSH model are SPT phases [22], we need to ensure that the error correction circuit cannot perform operations that violate these symmetries [9]. For example, performing an operation that corrects a single $|+\rangle$ error directly to the $|-\rangle$ state would be a violation of the chiral symmetry. A further minor complication arises due to the fact that phase errors $|+\rangle$ can arise as higher-order processes from density errors. This requires to correct phase errors before density errors, as otherwise correcting the density errors first can lead to dangling phase errors, which manifest themselves as spuriously diverging circuit depths. Taking these considerations into account, we arrive at the error correction procedure depicted in Fig. 1b: (i) We assign a walker to each measured error that searches its surrounding sites for the presence of other errors, switching between left and right with increasing distance from the initial position [9]. (ii) Phase errors get corrected by either fusing them pairwise or with a particle-hole error. (iii) Finally, density errors are corrected by fusing particles and holes. The depth of the circuit is then given by the total number of steps required to correct the system to the reference state.

Monte-Carlo sampling of matrix product states.— As the circuit depth corresponds to a highly nontrivial string operator, it is prohibitive to compute its expectation value from the exact solution of the model. Therefore, we turn to MPS calculations of the ground state using the ITensor library [23] up to $N = 100$ sites. However, even within a matrix product state formalism, efficient computation of arbitrary string operator expectation values is in general impossible, we turn to a Monte-Carlo sampling of the error measurements instead [24]. For this, we

start with a MPS $|\psi\rangle$ by calculating the probabilities to measure any of the basis states of the error basis $|\alpha\rangle_{1,2}$ of the first unit cell in terms of the expectation value of the associated projection operators $P_\alpha = |\alpha\rangle\langle\alpha|$. Subsequently, we draw a uniformly distributed random number to select the measurement result according to the probabilities $\langle P_\alpha \rangle$. Denoting the measurement result by $\alpha_{1,2}$, we can update the MPS according to $|\psi'\rangle = \mathcal{N}P_{\alpha_{1,2}}|\psi\rangle$, with \mathcal{N} referring normalization of the MPS, yielding the MPS conditional on the measurement result. Continuing the procedure over the entire system results in a string $\alpha_{1,2}\alpha_{2,3}\dots$ of the entire error configuration. Sampling over a large number of measurement outcomes and calculating the circuit depth for each outcome will then lead to an accurate estimation of the mean circuit depth or higher order moments such as the standard deviation.

Figure 1c shows the behavior of the circuit depth for the non-interacting SSH model. Here, we focus on the standard deviation σ of the depth as it exhibits slightly better finite scaling results. Due to the $v \leftrightarrow w$ symmetry of the model, it is sufficient to study only. We clearly see a divergence of the circuit depth around the critical value of $v/w = 1$, signaling the phase transition. Furthermore, finite size scaling reveals the critical point as $v_c/w = 1.00(1)$, i.e., the error correction procedure reproduces the quantitatively correct result.

Open boundary conditions.— So far, we have discussed the SSH model in the context of periodic boundary conditions. However, most interest in the SSH model lies in the realization of open boundary conditions due to the appearance of robust edge modes capable to store quantum information [15]. Implementation of the necessary error correction circuits can be done in a straightforward way from the periodic case. However, the possible degeneracy implies that the parity of the ground state is not well-defined. Therefore, we ignore the state of the two edge spins in the case of $|\psi_{AB}\rangle$ as the reference state.

Figure 2 shows the MPS simulation results for both

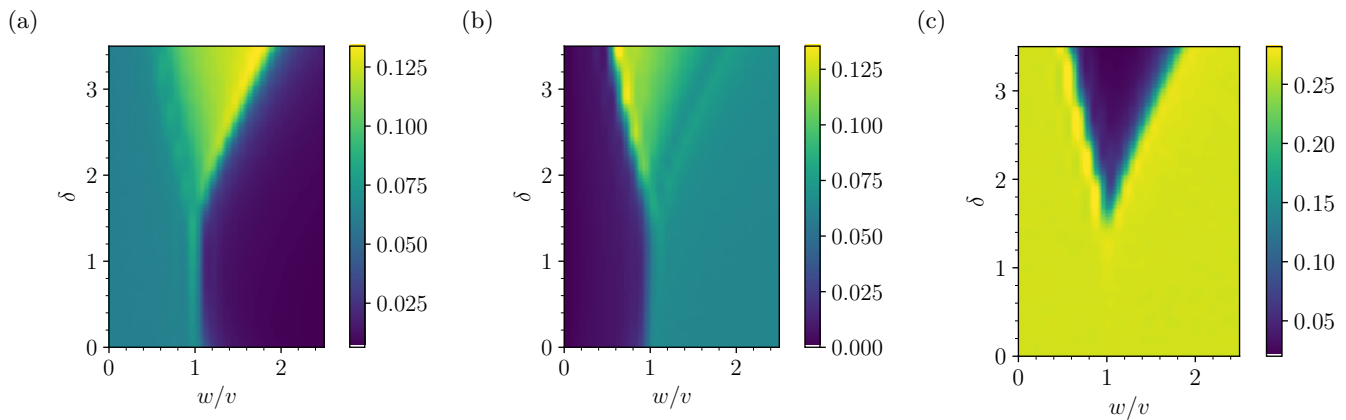


FIG. 3. Phases of the extended SSH model, calculated by the circuit depth to correct the ground state to the two SPT ordered reference states $|\psi_{AB}\rangle$ (a) and $|\psi_{BA}\rangle$ (b), as well as to the antiferromagnetic state $|\psi_{AF}\rangle$ (c) for $N = 100$ sites. The dark areas indicate a vanishing of the normalized circuit depth σ/N , showing that the ground state is in the same phase as the reference state. All areas of short circuit depths are mutually exclusive and span the entire parameter range.

reference states $|\psi_{AB}\rangle$ and $|\psi_{BA}\rangle$. As in the case of periodic boundary conditions, we observe a phase transition between the two phases at $v/w = 1$. However, since the introduction of open boundaries breaks the $v \leftrightarrow w$ symmetry, the identification of both phases as SPT phases deserves further discussion. For the $v < w$, this identification is straightforward, as the edge mode can be used to encode a topological qubit, whose logical state is preserved under the error correction circuit. However, this argument does not hold for $v > w$ as the ground state is unique. Nevertheless, we can establish the phase being SPT ordered by inspecting the reference state $|\psi_{BA}\rangle$. Since the reference state is a product state of all unit cells, it is sufficient to look at a single unit cell. A state is SPT ordered, if there is no set of symmetry-preserving local unitaries that transform the state into a product state [25]. To identify the possible unitaries on a single unit cell, we note that all accessible states have to be in the same symmetry sector as the $|-\rangle$ state with respect to the chiral symmetry and the $U(1)$ symmetry corresponding to particle number conservation [22]. Crucially, there is no other state that fulfills these criteria. This means that there is no symmetry-preserving circuit that can transform the state $|\psi_{BA}\rangle$ to a product state and hence this phase must be SPT ordered.

Additionally, it is instructive to look at the effective low energy Hamiltonian (3) again to obtain insight into the breaking of the ground state degeneracy by the topological phase transition [26]. For this, we consider the effective Hamiltonian on the first site of the lattice, which in a mean-field decoupling is given by $H_1 = vS_1^-\langle S_2^+\rangle + \text{H.c.}$. Within a mean-field decoupling, $\langle S_2^+\rangle$ is nonzero only for $v > w$, opening a gap between the edge modes above the transition. While this simple mean-field decoupling is unable to correctly describe the Haldane insulator, one can expect that this argument

also holds within a more refined treatment [27].

Figs/ Extended SSH model.— Let us now go beyond the noninteracting case and study an extension of the SSH model including antiferromagnetic interactions [7], given by the Hamiltonian

$$H = H_0 + \frac{\delta}{2} \left[v \sum_{i=1}^{N/2} \sigma_z^{2i-1} \sigma_z^{2i} + w \sum_{i=1}^{N/2-1} \sigma_z^{2i} \sigma_z^{2i+1} \right]. \quad (5)$$

While we discuss the bosonic version of the model here, we would like to note that one can also study an equivalent fermionic version including a chemical potential and a nearest-neighbor interaction, where the chemical potential is tuned such that the particle-hole symmetry of the SSH model is preserved.

In the limit of large δ , it is evident that the terms in H_0 are irrelevant and the ground state is an Ising antiferromagnet. It is easy to construct a reference state for this phase, as it is simply a classical state $|\psi_{AF}\rangle = |010101\dots\rangle$. Errors are given by domain wall excitations located on the bonds between two sites occurring when the spin state of these sites is identical. Local spin flips always create these excitations in pairs, hence the error correction is given by the pairwise fusion of all domain walls. Note that in contrast to the previous reference state, we have only one elementary excitation instead of two. This can be attributed to the fact that an Ising antiferromagnet can only reliably store *classical* information, while the edge mode in the SSH model can store *quantum* information, i.e., while an Ising antiferromagnet can correct bit-flip errors, it does not correct phase errors.

In Figure 3, we show the error correction properties of the extended SSH model as a function of w/v and δ for all three reference states $|\psi_{BA,AB,AF}\rangle$. We can clearly see that the areas of short circuit depths are mutually

exclusive and span the entire parameter range, i.e., the error correction approach can be successfully employed to determine the complete phase diagram. Additionally, the phase boundaries are in excellent quantitative agreement with those obtained using an approach based on the application of random quantum gates [7].

In summary, we have explored the phase diagram of an interacting topological insulator model based on the error correction properties of the ground state. We show that this approach can successfully map out the entire phase diagram, including the transition to an antiferromagnetic phase exhibiting spontaneous symmetry breaking. Finally, the operational character based on measurable observables enables to directly detect topological order in future experimental studies.

We thank S. Diehl, P. Recher, and B. Vermersch for fruitful discussions. This work was funded by the Volkswagen Foundation, by the Deutsche Forschungsgemeinschaft (DFG, German Research Foundation) within SFB 1227 (DQ-mat, project A04), SPP 1929 (GiRyd), and under Germany's Excellence Strategy – EXC-2123 QuantumFrontiers – 390837967.

* amit.jamadagni@itp.uni-hannover.de

- [1] D. J. Thouless, M. Kohmoto, M. P. Nightingale, and M. den Nijs, Quantized Hall Conductance in a Two-Dimensional Periodic Potential, *Phys. Rev. Lett.* **49**, 405 (1982).
- [2] M. Kohmoto, Topological invariant and the quantization of the Hall conductance, *Ann. Phys. (N. Y.)* **160**, 343 (1985).
- [3] A. Kitaev, Periodic table for topological insulators and superconductors, *AIP Conf. Proc.* **1134**, 22 (2009).
- [4] L. Fidkowski and A. Kitaev, Effects of interactions on the topological classification of free fermion systems, *Phys. Rev. B* **81**, 134509 (2010).
- [5] J. Haegeman, D. Pérez-García, I. Cirac, and N. Schuch, Order Parameter for Symmetry-Protected Phases in One Dimension, *Phys. Rev. Lett.* **109**, 050402 (2012).
- [6] F. Pollmann and A. M. Turner, Detection of symmetry-protected topological phases in one dimension, *Phys. Rev. B* **86**, 125441 (2012).
- [7] A. Elben, J. Yu, G. Zhu, M. Hafezi, F. Pollmann, P. Zoller, and B. Vermersch, Many-body topological invariants from randomized measurements in synthetic quantum matter, *Science Adv.* **6** (2020).
- [8] X. Chen, Z.-C. Gu, and X.-G. Wen, Complete classification of one-dimensional gapped quantum phases in interacting spin systems, *Phys. Rev. B* **84**, 235128 (2011).
- [9] A. Jamadagni and H. Weimer, An Operational Definition of Topological Order, [arXiv:2005.06501](https://arxiv.org/abs/2005.06501) (2020).
- [10] A. Y. Kitaev, Fault-tolerant quantum computation by anyons, *Ann. Phys. (N. Y.)* **303**, 2 (2003).
- [11] A. Y. Kitaev, Unpaired Majorana fermions in quantum wires, *Phys.-Usp.* **44**, 131 (2001).
- [12] M. Leijnse and K. Flensberg, Introduction to topological superconductivity and Majorana fermions, *Semicond. Sci. Technol.* **27**, 124003 (2012).
- [13] S. D. Sarma, M. Freedman, and C. Nayak, Majorana zero modes and topological quantum computation, *npj Quantum Inf.* **1**, 15001 (2015).
- [14] W. Su, J. Schrieffer, and A. Heeger, Soliton excitations in polyacetylene, *Phys. Rev. B* **22**, 2099 (1980).
- [15] J. K. Asbóth, L. Oroszlány, and A. Pályi, *A Short Course on Topological Insulators*, Lecture Notes in Physics, Vol. 919 (Springer International Publishing, Cham, 2016).
- [16] S. de Léséleuc, V. Lienhard, P. Scholl, D. Barredo, S. Weber, N. Lang, H. P. Büchler, T. Lahaye, and A. Browaeys, Observation of a symmetry-protected topological phase of interacting bosons with Rydberg atoms, *Science* **365**, 775 (2019).
- [17] S. Trebst, P. Werner, M. Troyer, K. Shtengel, and C. Nayak, Breakdown of a Topological Phase: Quantum Phase Transition in a Loop Gas Model with Tension, *Phys. Rev. Lett.* **98**, 070602 (2007).
- [18] L. Tagliacozzo and G. Vidal, Entanglement renormalization and gauge symmetry, *Phys. Rev. B* **83**, 115127 (2011).
- [19] O. Golinelli, T. Jolicoeur, and R. Lacaze, Dispersion of magnetic excitations in a spin-1 chain with easy-plane anisotropy, *Phys. Rev. B* **46**, 10854 (1992).
- [20] W. Chen, K. Hida, and B. C. Sanctuary, Ground-state phase diagram of $S = 1$ XXZ chains with uniaxial single-ion-type anisotropy, *Phys. Rev. B* **67**, 104401 (2003).
- [21] Z.-C. Gu and X.-G. Wen, Tensor-entanglement-filtering renormalization approach and symmetry-protected topological order, *Phys. Rev. B* **80**, 155131 (2009).
- [22] T. Micallo, V. Vitale, M. Dalmonte, and P. Fromholz, Topological entanglement properties of disconnected partitions in the Su-Schrieffer-Heeger model, *SciPost Phys. Core* **3**, 12 (2020).
- [23] M. Fishman, S. R. White, and E. M. Stoudenmire, The ITensor Software Library for Tensor Network Calculations, [arXiv:2007.14822](https://arxiv.org/abs/2007.14822) (2020).
- [24] Z.-Y. Han, J. Wang, H. Fan, L. Wang, and P. Zhang, Unsupervised Generative Modeling Using Matrix Product States, *Phys. Rev. X* **8**, 031012 (2018).
- [25] X. Chen, Z.-C. Gu, and X.-G. Wen, Local unitary transformation, long-range quantum entanglement, wave function renormalization, and topological order, *Phys. Rev. B* **82**, 155138 (2010).
- [26] A. Jamadagni, H. Weimer, and A. Bhattacharyya, Robustness of topological order in the toric code with open boundaries, *Phys. Rev. B* **98**, 235147 (2018).
- [27] T. Kennedy and H. Tasaki, Hidden $Z_2 \times Z_2$ symmetry breaking in Haldane-gap antiferromagnets, *Phys. Rev. B* **45**, 304 (1992).